Preamble Detection in NB-IoT Random Access with Limited-Capacity Backhaul

Hien, Ta Quang; Wang, Zhengdao; Kim, Sang W.; Nielsen, Jimmy Jessen; Popovski, Petar

Published in:
2019 IEEE International Conference on Communications, ICC 2019 - Proceedings

DOI (link to publication from Publisher):
10.1109/ICC.2019.8761284

Publication date:
2019

Document Version
Accepted author manuscript, peer reviewed version

Preamble Detection in NB-IoT Random Access with Limited-Capacity Backhaul

Hien Q. Ta*, Zhengdao Wang*, Sang W. Kim*, Jimmy J. Nielsen†, Petar Popovski†
* Dept. of Electrical and Computer Engineering, Iowa State University, Ames, Iowa, USA 50011
Email: {hienta, zhengdao, swkim}@iastate.edu
† Dept. of Electronic Systems, Aalborg University, 9220 Aalborg, Denmark
Email: {jjn, petarp}@es.aau.dk

***Abstract*—We study multi-base station (BS) preamble detection schemes for the narrow-band Internet of Things (NB-IoT) random access by using stochastic geometry analysis. Specifically, we compare the preamble detection performance of two baseline detection schemes: Quantize-and-Forward (QnF) and Detect-and-Forward (DnF). QnF requires the feedback of quantized received power levels while DnF requires 1-bit feedback of local detection result. Our results show that DnF scheme outperforms QnF scheme when the backhaul capacity is limited or when the minimum distance between user and BSs is less than a threshold. Our results also show that the use of multiple collaborative BSs can lead to a significant improvement of the preamble detection performance, as well as reduction of the total power of the preamble transmission.**

***Index Terms*—NB-IoT, Random Access, Preamble Detection.**

I. Introduction

Internet of Things (IoT) plays an important role in the future wireless network where everything will be connected [1]. There are two classes of IoT transmission technologies, low-power wide-area (LPWA) and cellular IoT. Generally, LPWA operate in an unlicensed spectrum, while cellular IoT in a licensed spectrum. Recently, NB-IoT in cellular IoT has been considered to be a promising technology that provides large coverage and low power consumption for low-throughput low-cost devices in delay-tolerant applications [2].

As an initial fundamental network function, random access aims to identity the set of active users and to establish resource allocation for transmissions. Different from LTE where random access design is centered on the Zadoff-Chu (ZC) orthogonal sequences [3], the set of othorgonal preamble sequences in NB-IoT physical random access channel (NPRACH) is designed with the aid of single-tone frequency hopping technique [2], [4]. To guarantee a certain preamble detection performance under low transmission power, transmission repetition is required in NB-IoT. Preamble detection in NB-IoT has been studied in [4]–[6]. More specifically, [4] firstly proposed algorithm to detect the preamble and estimate the time of arrival (TOA) simultaneously. [5] improved the TOA estimation by modifying the hopping pattern that all possible hopping distances can be fully used for a given number of subcarriers. Finally, [6] proposed the partial preamble transmission and characterizes the trade-off between the preamble detection performance and collisions.

Recently, the user activity detection has been improved by having massive antennas in massive multiple-input multiple-output (MIMO) system [7] or having multiple base stations (BSs) in C-RAN system with limited-capacity fronthaul [8] in context of grant-free random access, where the non-orthogonal preamble sequences are used. The basic idea is to utilize the spatial diversity at receiver side to improve detection. Inspired by these ideas, our paper considers collaborative detection with multiple BSs in context of NB-IoT grant-based random access. To the best of our knowledge, the impact of multiple BSs on the preamble detection has not been studied for NB-IoT.

Furthermore, stochastic geometry is a useful tool for characterizing the spatial distribution of users and BSs [9]. In this paper, we, therefore, study the NB-IoT preamble detection with multiple BSs using stochastic geometry analysis. The contributions of this paper is summarized as follows:

- We derive the missed detection probability under fixed false alarm probability for the QnF and DnF schemes, and compare two schemes under limited-capacity backhaul and different scales of the network.
- We show that DnF outperforms QnF when the backhaul capacity is limited or the minimum distance between user and BSs is less than a threshold.
- We also show that the use of multiple collaborative BSs can lead to a significant improvement of the preamble detection performance as well as reduction of the total power of the preamble transmission.

The remaining part of the paper is organized as follows. Section II describes the system model. Section III discusses the preamble detection strategy and derives the missed detection probability of the Quantize-and-Forward and Detect-and-Forward schemes. Section IV optimizes total power of the preamble transmission and Section VI concludes the paper.

II. System Model

We consider a system model where K BSs jointly detect users' activity. We assume that K BSs are each equipped with single antenna[1] and are connected to a centralized unit (CU) via error-free backhaul links, and that the BSs are uniformly distributed on the two-dimensional Euclidean plane.

Let R denote the distance in meters from a user to the farthest BS and let r ($1 \leq r \leq R$) denote the distance in meters from a user to the closest BS, where r is required larger than or equal to 1 as following the bounded pathloss model [10]. Then, the network system of the user and K BSs can be seen as the ring-shaped region (annulus) centered at the user with inner radius r and outer radius R, which can be shown in Fig.1. When there is no collaboration of BSs, i.e. single-BS case, the user should be associated with the closest

[1]An extension of multiple antennas will be considered in future work.

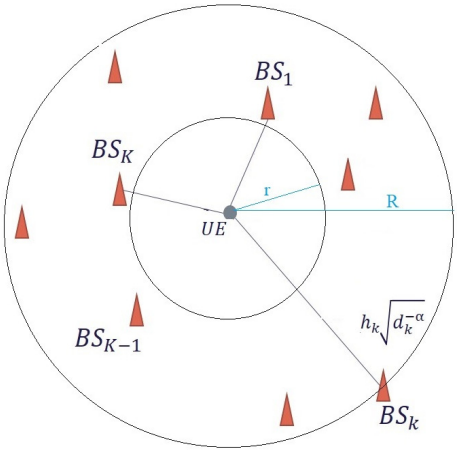

Fig. 1. System Configuration

BS and the ring-shaped region reduces to the circle line with radius r, where r is usually in the range of kilometers for NB-IoT applications [4]. Note that each user has a different value of r and R.

A. Preamble Structure

The preamble sequence consists of M_p repetitions. Each replica has v symbol groups which each symbol group is composed of a cyclic prefix (CP) and ξ symbols. The preamble sequence consists of fixed-size frequency hopping in each repetition, and pseudo-hopping among repetitions dependent on cell identity and repetition index. The former is designed for the BS to estimate TOA while the latter is to avoid persistent interference between different cells [2]. This unique design of preamble sequence is known at the BSs.

B. Preamble Transmission

At preamble transmission phase, each user chooses a random index and transmits the preamble sequence corresponding to the chosen index. The transmitted preamble signal is $\sqrt{P}x_{m,j,i}$, where P denotes the transmit power and $x_{m,j,i}$ denotes the normalized i-th transmitted symbol in j-th symbol group at m-th repetition.

Since narrow band signal is considered in NB-IoT, the random access channel can be modeled as a single-tap channel. We assume that the channel does not vary in one symbol group but varies independently among symbol groups[2], and that the channel between a user and k-th BS at m-th repetition can be modeled as $h_{m,j}^{(k)}\sqrt{d_k^{-\alpha}}$ for $k \in \{1,...,K\}$ and $m \in \{1,...,M_p\}$, where $h_{m,j}^{(k)} \sim CN(0,1)$ is the small-scale fading and $d_k^{-\alpha}$ is the large scale fading with path-loss exponent α ($\alpha > 2$) and distance d_k, where d_k has the probability density function (PDF) [11],

$$f_d(x) = 2x/(R^2 - r^2), \ r \le x \le R. \tag{1}$$

[2]In NB-IoT, since the number of symbols in one symbol group is designed to be small such that the channel variation is negligible [4], the assumption is reasonable under consideration.

We assume that a user knows the information[3] of r and R, and receives the information of the total number of collaborative BSs, K, via the master information block (MIB) downlink signal. Hence, by knowing r, R and K, the user can adapt its transmission power to guarantee a given detection performance similar to the single-BS case where the user adapts the transmission power to compensate the large-scale pathloss [2]. It should be noted that the BSs do not know the location of the user at the preamble transmission phase.

C. Received Power at BSs

The received signal at k-th BS is given by

$$y_{m,j,i}^{(k)} = \sqrt{Pd_k^{-\alpha}}h_{m,j}^{(k)}x_{m,j,i} + n_{m,j,i}^{(k)}, \tag{2}$$

for $k \in \{1,...,K\}$, where $n_{m,j,i}^{(k)}$ denotes complex Gaussian noise with zero mean and variance σ_n^2. Then, power delay profile (PDP) is computed by correlating the known preamble sequence and the received signal as a function of propagation delay. Hence, the peak value of PDP, which the round-trip delay, i.e. time of arrival (TOA), is estimated, at k-th BS is given by [4]

$$J_k(P) = \sum_{m=1}^{M_p}\left|\sum_{j=1}^{v}\sum_{i=1}^{\xi} r_{m,j,i}^{(k)}\right|^2, \tag{3}$$

where $r_{m,j,i}^{(k)} = y_{m,j,i}^{(k)}x_{m,j,i}^{(k)*} = \sqrt{Pd_k^{-\alpha}}h_{m,j}^{(k)} + \tilde{n}_{m,j,i}^{(k)}$ is the correlation between $x_{m,j,i}^{(k)}$ and $y_{m,j,i}^{(k)}$, and $\tilde{n}_{m,j,i}^{(k)}$ has the same distribution as $n_{m,j,i}^{(k)}$.

Let $\gamma = P/\sigma_n^2$ denote the transmit signal-to-noise ratio (SNR). Then for given d_k

$$J_k(\gamma) = \sum_{m=1}^{M_p}\left|\sum_{j=1}^{v}\xi\sqrt{Pd_k^{-\alpha}}h_{m,j}^{(k)} + \sum_{j=1}^{v}\sum_{i=1}^{\xi}\tilde{n}_{m,j,i}^{(k)}\right|^2 \tag{4}$$

has gamma distribution with shape M_p and scale $v\xi\sigma_n^2(1+\xi\gamma d_k^{-\alpha})$, $J_k(\gamma) \sim \text{Gamma}(M_p, v\xi\sigma_n^2(1+\xi\gamma d_k^{-\alpha}))$ [6], i.e.

$$f_{J_k}(x|d_k) = \frac{x^{M_p-1}e^{-\frac{x}{v\xi\sigma_n^2(1+\xi\gamma d_k^{-\alpha})}}}{(M_p-1)!(v\xi\sigma_n^2(1+\xi\gamma d_k^{-\alpha}))^{M_p}}. \tag{5}$$

III. Preamble Detection

In this section, we consider two baseline schemes, named Quantize-and-Forward detection (QnF) and Detect-and-Forward detection (DnF). Different from the grant-free random access [8] where it requires feedback per each repetition, our paper requires one-time feedback after all transmission repetitions. Hence, the number of feedback information in [8] depends on the number of repetition, whereas the number of feedback information in our paper is independent of the number of repetitions.

Under the limited-capacity backhaul, different from [8] where a trade off between the number of repetition and the

[3]The assumption is suitable for such scenarios when the largest and smallest distance, R and r, can be estimated from downlink signals, or when users are in fixed locations and their distance to BSs is constant and is known at each node.

quantization bits is considered, our paper consider a trade off between the number of collaborating BSs and the quantization bits. Especially for the DnF scheme, where 1-bit feedback is used, the total number of collaborating BSs must not exceed the backhaul capacity.

A. Quantize-and-Forward

With QnF, each BS quantizes the peak value of PDP, e.g. $J_k(\gamma)$ at k-th BS, and sends the quantized power to CU where a detection is performed[4]. The peak value of PDP is quantized with a positive integer value of b bits per sample, i.e. the received power at CU from the k-th BS can be written as [8]

$$\hat{J}_k(\gamma) \quad = \quad \mathcal{Q}(J_k(\gamma)), \tag{6}$$

where $\mathcal{Q}$ is a quantization function. Since the information of large-scale fading is not available at BSs, an optimal quantizer at BSs as in [8] is impossible. Instead, a simple uniform quantizer is considered.

1) Detection Rule: Since the information of the large-scale fading is not available at BSs, the equal gain combining (EGC) detection is used at CU [12], i.e.,

$$\sum_{k=1}^{K} \hat{J}_k(\gamma) \underset{\mathcal{D}_0}{\overset{\mathcal{D}_1}{\gtrless}} \lambda_{QnF}, \tag{7}$$

where the quantized received power of (6) under the uniform quantizer at BSs can be rewritten as

$$\hat{J}_k(\gamma) = J_k(\gamma) + e_k, \text{ for } 1 \le k \le K, \tag{8}$$

where e_k is the quantization error independent with $J_k(\gamma)$ and has uniform distribution, $U(-\Delta/2, \Delta/2)$, where $\Delta = 2^{-b}P_{max}$, and P_{max} is the maximum power chosen to be equal to λ_{QnF}. Thereby, if any BS receives power larger than λ_{QnF}, the detection result of (7) will be $\mathcal{D}_1$.

Let $S(\gamma) := \sum_{k=1}^{K} J_k(\gamma)$ denote the total received powers from all BSs. It follows from [10] and [13] that the distribution of $S(\gamma)$ can be approximated as gamma distribution[5] with shape $c := \mathrm{E}[S(\gamma)]^2/\mathrm{var}[S(\gamma)]$ and scale $d := \mathrm{var}[S(\gamma)]/\mathrm{E}[S(\gamma)]$, i.e. $S(\gamma) \sim \text{Gamma}(c, d)$. The mean of $S(\gamma)$ is given by

$$\mathrm{E}[S(\gamma)] = KM_p v\xi\sigma_n^2 \left(1 + 2\xi\gamma \frac{(r^{2-\alpha} - R^{2-\alpha})}{(\alpha-2)(R^2 - r^2)}\right), \tag{9}$$

and the variance of $S(\gamma)$ is given by

$$\begin{aligned}\mathrm{var}[S(\gamma)] = {} & KM_p(v\xi\sigma_n^2)^2 \left(1 + 4\xi\gamma \frac{(r^{2-\alpha} - R^{2-\alpha})}{(\alpha-2)(R^2 - r^2)}\right) \\ & + K(v\xi\sigma_n^2)^2(\xi\gamma)^2 \Bigg(\frac{(M_p^2 + M_p)(r^{2-2\alpha} - R^{2-2\alpha})}{(\alpha-1)(R^2 - r^2)} \\ & - \frac{4M_p^2(r^{2-\alpha} - R^{2-\alpha})^2}{(\alpha-2)^2(R^2 - r^2)^2} \Bigg).\end{aligned} \tag{10}$$

The derivation of (9) and (10) is provided in Appendix A.

[4]Note that the detection of preamble transmission based on feedbacks of the received powers does not affect the estimation of TOA at each BS.

[5]Since [13] and [10] showed the high accuracy of gamma distribution approximation for $S(\gamma)$ for $K \ge 6$, our paper simply applies this approximation result into the analysis.

Let $Y := \sum_{k=1}^{K} (e_k/\Delta + 0.5)$ denote the sum of i.i.d normalized uniform distribution, $U(0,1)$, i.e. Y has Irwin-Hall distribution,

$$f_Y(y) = \sum_{j=0}^{K} (-1)^j \binom{K}{j} \frac{(y-j)^{K-1}}{2(K-1)!} \mathrm{sgn}(y-j) \tag{11}$$

for $0 \le y \le K$, where $\mathrm{sgn}(y-j)$ is the sign function,

$$\mathrm{sgn}(y-j) = \begin{cases} -1, & y < j, \\ 0, & y = j, \\ 1, & y > j. \end{cases} \tag{12}$$

Hence, the LHS of (7) can be rewritten as

$$\sum_{k=1}^{K} \hat{J}_k(\gamma) = S(\gamma) + Y\Delta - K\Delta/2. \tag{13}$$

2) Missed detection probability: Since $S(0) \sim \text{Gamma}(KM_p, v\xi\sigma_n^2)$, the false alarm probability for given λ_{QnF} can be obtained as

$$\begin{aligned} & P_{f,QnF}(b,K) \\ & = \Pr\left(\sum_{k=1}^{K} \hat{J}_k(0) > \lambda_{QnF} \middle| \mathcal{D}_0\right) && (14) \\ & = \Pr\left(S(0) + Y\Delta - K\Delta/2 > \lambda_{QnF}\right) && (15) \\ & = 1 - \Pr\left(S(0) + Y\Delta \le \lambda_{QnF} + K\Delta/2\right) && (16) \\ & = 1 - \int_0^{\frac{\lambda_{QnF}}{\Delta} + \frac{K}{2}} f_Y(y)dy\Gamma\left(KM_p, \frac{\lambda_{QnF} + K\Delta/2 - y\Delta}{v\xi\sigma_n^2}\right) && (17) \end{aligned}$$

where $\Gamma(n,x) = \int_0^x \frac{t^{n-1}e^{-t}}{(n-1)!}dt$ is the generalized incomplete Gamma function, and the integral part of (17) can be computed by Trapezoid method.

Since $S(\gamma) \sim \text{Gamma}(c,d)$, the missed detection probability for given λ_{QnF} can also be obtained by, similar to (17),

$$\begin{aligned} & P_{m,QnF}(b,K) \\ & = \Pr\left(\sum_{k=1}^{K} \hat{J}_k(\gamma) < \lambda_{QnF} \middle| \mathcal{D}_1\right) && (18) \\ & = \Pr\left(S(\gamma) + Y\Delta < \lambda_{QnF} + K\Delta/2\right) && (19) \\ & = \int_0^{\frac{\lambda_{QnF}}{\Delta} + \frac{K}{2}} f_Y(y)dy\Gamma\left(c, \left(\lambda_{QnF} + K\Delta/2 - y\Delta\right)/d\right). && (20) \end{aligned}$$

Therefore, for $P_{f,QnF}(b,K) = P_f$, we can obtain the detection threshold, λ_{QnF}, from (17) and then, the missed detection probability, $P_{m,QnF}(b,K)$, from (20).

Remark 1: Due to the nature of limited-capacity backhaul,

$$b \times K \le C_f, \tag{21}$$

where C_f (bits/use) represents the limited-capacity backhaul, it is possible to trade the number of collaborated BSs for the number of bits per sample to minimize the missed detection probability. Therefore, the missed detection probability of the QnF scheme is given by

$$P_{m,QnF} = \min_{b \times K \le C_f} P_{m,QnF}(b,K). \tag{22}$$

Special case: When r goes to 1 for given large R ($r/R \to 0$), we have

$$\frac{r^{2-\alpha} - R^{2-\alpha}}{R^2 - r^2} = r^{-\alpha}\left(\frac{r}{R}\right)^2 \frac{1-(r/R)^{\alpha-2}}{1-(r/R)^2} \to 0, \quad (23)$$

and similarly,

$$\frac{r^{2-2\alpha} - R^{2-2\alpha}}{R^2 - r^2} \to 0. \quad (24)$$

It follows from (9) and (10) that the mean and variance of $S(\gamma)$ converge to

$$\begin{aligned} \mathrm{E}[S(\gamma)] &\to KM_p v\xi\sigma_n^2, & (25)\\ \mathrm{var}[S(\gamma)] &\to KM_p(v\xi\sigma_n^2)^2, & (26) \end{aligned}$$

respectively. Then, we obtain from (25) and (26) that $S(\gamma) \sim \mathrm{Gamma}(KM_p, v\xi\sigma_n^2)$, which is the same distribution of $S(0)$ for no preamble transmission case. It is because the density of BSs converges to zero and then the summing power of received information-bearing signals goes to zero.

Hence, it follows from (17) and (20) that $P_{f,QnF}(b,K) + P_{m,QnF}(b,K) \to 1$. Therefore, the missed detection probability approaches 1 if the false alarm probability is forced to approach 0.

B. Detect-and-Forward

With DnF, each BS individually detects the preamble transmission and sends the detection result to CU. Since the observation of BSs are i.i.d, each BS chooses the same detection threshold, i.e. the detection at BSs is

$$J_k(\gamma) \underset{\mathcal{D}_0^k}{\overset{\mathcal{D}_1^k}{\gtrless}} \lambda_{DnF}, \ 1 \le k \le K, \quad (27)$$

where λ_{DnF} is the detection threshold, and $\mathcal{D}_0^k$ and $\mathcal{D}_1^k$ denote the hypothesis of no preamble transmission and preamble transmission at k-th BS, respectively. Since each BS is required to send the detection result to CU, a BS can implement the 1-bit feedback process without error, which is "1" if $\mathcal{D}_1^k$, and "0" if $\mathcal{D}_0^k$.

Since CU does not know the large-scale fading, CU will apply the *majority voting* rule to have final decision [14]; that is, if CU receives more than half of "1" feedbacks, there is a preamble transmission and, otherwise, there is no preamble transmission. Hence, the false alarm probability for given λ_{DnF} is given by [14]

$$\begin{aligned} P_{f,DnF} &= \sum_{i=\lfloor K/2\rfloor+1}^{K} \binom{K}{i} \left[\Pr(J_i(0) > \lambda_{DnF}|\mathcal{D}_0^i)\right]^i \\ &\quad \times \left[1 - \Pr(J_i(0) > \lambda_{DnF}|\mathcal{D}_0^i)\right]^{K-i} \quad (28)\\ &= \sum_{i=\lfloor K/2\rfloor+1}^{K} \binom{K}{i} \left[1 - \Gamma\left(M_p, \frac{\lambda_{DnF}}{v\xi\sigma_n^2}\right)\right]^i \\ &\quad \times \left[\Gamma\left(M_p, \frac{\lambda_{DnF}}{v\xi\sigma_n^2}\right)\right]^{K-i}. \quad (29) \end{aligned}$$

where $\lfloor x \rfloor$ is the largest integer smaller than or equal to x.

For $P_{f,DnF} = P_f$, λ_{DnF} can be numerically computed from (29). Then, the missed detection probability can be obtained by

$$\begin{aligned} P_{m,DnF} &= 1 - \sum_{i=\lfloor K/2\rfloor+1}^{K} \binom{K}{i} \left[\Pr(J_i(\gamma) > \lambda_{DnF}|\mathcal{D}_1^i)\right]^i \\ &\quad \times \left[1 - \Pr(J_i(\gamma) > \lambda_{DnF}|\mathcal{D}_1^i)\right]^{K-i}, \quad (30) \end{aligned}$$

where from (1) and (5),

$$\begin{aligned} &\Pr(J_i(\gamma) > \lambda_{DnF}|\mathcal{D}_1^i) \\ &= \int_r^R \Pr(J_i(\gamma) > \lambda_{DnF}|\mathcal{D}_1^i, d_i) f_d(x) dx \quad (31)\\ &= 1 - \int_r^R \Gamma\left(M_p, \frac{\lambda_{DnF}}{v\xi\sigma_n^2(1+\xi\gamma x^{-\alpha})}\right) \frac{2x}{R^2 - r^2} dx \quad (32) \end{aligned}$$

can be computed by Trapezoid method.

It is shown in Appendix B that $\Pr(J_i(\gamma) > \lambda_{DnF}|\mathcal{D}_1^i)$ is a strictly decreasing function of r. Also, it can be shown that $P_{m,DnF}$ in (30) is a strictly increasing function of $\Pr(J_i(\gamma) > \lambda_{DnF}|\mathcal{D}_1^i)$. Hence, the missed detection probability of the DnF scheme is an increasing function of r.

It is interesting that when r goes to 1 for given large R, i.e. $r/R \to 0$, and $P_f \ll 1$, the detection performance of the DnF scheme is minimized while that of the QnF scheme is maximized (goes to 1), which can be shown in Figure 2.

Remark 2: For limited-capacity backhaul, since DnF scheme requires 1-bit feedback without error, the constraint of (21) in DnF scheme reduces to $K \le C_f$.

C. Numerical Results

Throughout the paper, missed detection probabilities in (20) and (30) are numerically computed via Trapezoid method, and the parameters are chosen as follows [2]: the effective noise power, σ_n^2, for the bandwidth 3.75 kHz is $10^{-16.53}$, the pathloss exponent, α, is 4 for typical macrocell urban channel, $v = 4$, and $\xi = 5$.

Figure 2 compares the detection performance of two schemes versus the inner radius, r, for different value of outer radius, R. It can be seen that the missed detection probability of both schemes decreases significantly as the outer bound R increases. It is because BSs located far from user have unreliable link, thus degrading the detection performance. It can also be seen that the DnF scheme outperforms the QnF scheme when the minimum distance between user and BSs, r, is less than a threshold. It is interesting that there exists an optimal r that minimizes the missed detection probability of the QnF scheme.

Figure 3 shows the missed detection probability versus the number of BSs, K, for the specific range, $r = 10$ Km and $R = 20$ Km, in favor of the QnF scheme (see Fig. 2). It can be seen that when there is limited-capacity backhaul, the detection performance of QnF converges as K increases and is not as good as that of DnF for large K. It is because the QnF scheme has high quantization noise for large K while the DnF scheme benefits from local detection at BSs without loss of feedback information as long as $K \le C_f$.

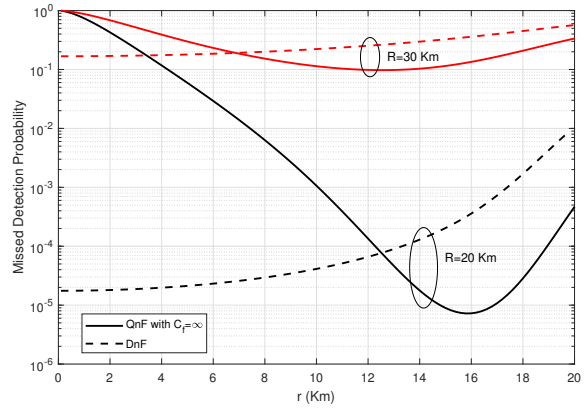

Fig. 2. Missed detection probability versus r for different value of R; $K = 5$, $M_p = 16$, $P_f = 10^{-3}$ and $P = 30$ dBm.

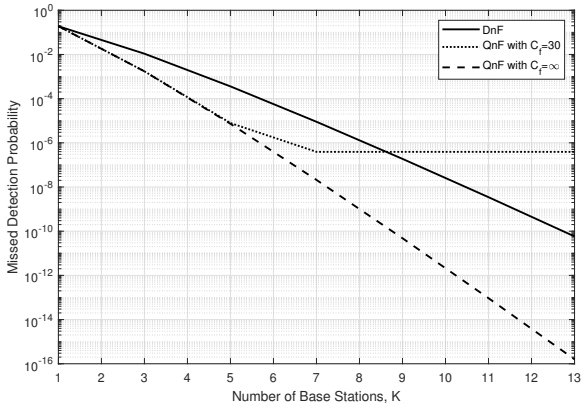

Fig. 3. Missed detection probability versus total number of BSs, K; $R = 20$ Km, $r = 16$ Km, $M_p = 16$, $P_f = 10^{-3}$ and $P = 30$ dBm.

IV. Minimum Total Transmission Power

In this section, we consider the problem of minimizing the total transmission power under constraint of transmission power per symbol and missed detection probability, i.e.

$$\min_{M_p,P} \quad P_{tot} = v\xi M_p P \tag{33}$$

$$\text{subject to :} \quad P \leq P_{\max} \tag{34}$$

$$P_{m,X} \leq \epsilon, \tag{35}$$

where $P_{\max}$ is the maximum allowed transmission power per symbol[6], ϵ is the target missed detection probability, and $P_{m,X}$ denote the missed detection probability of scheme X.

It can be seen from (33) that M_p with integer value has a dominant impact on the total transmission power, P_{total}. The problem of (33)-(35) can be solved with numerical search. That is, we firstly fix $P = P_{\max}$ and find the minimum number of repetition, M_p^*, satisfying the constraint of (35). Then, we find the minimum P^* also satisfying the constraint of (35) when $M_p = M_p^*$. Hence, the minimum total transmission power will be given by $v\xi M_p^* P^*$.

[6]NB-IoT device is low-cost and low-throughput with limitations of hardware. Hence, a constraint of transmission power per symbol is necessary.

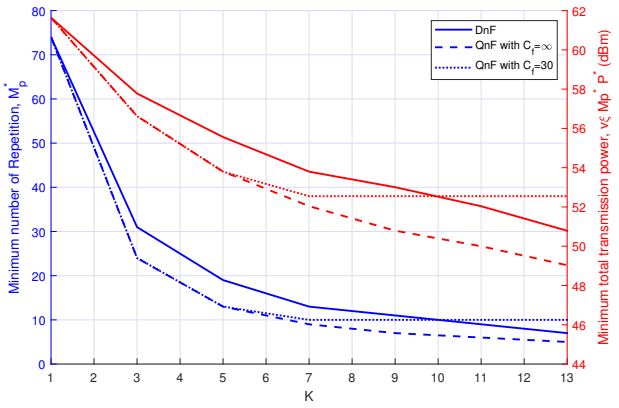

Fig. 4. The minimum total transmission power (red color) and the minimum number of repetition (blue color) versus total number of BSs, K, for different values of C_f; $R = 20$ Km, $r = 16$ Km, $P_f = 10^{-3}$, $\epsilon = 10^{-3}$, and $P_{max} = 30$ dBm.

Figures 4 shows the minimum total transmission power (red color) and the minimum number of repetition (blue color) versus the number of BSs, K. It can be seen that the total transmission power and number of repetition of the DnF scheme and the QnF scheme with sufficient-capacity backhaul decreases significantly and monotonically as the number of collaborating BSs, K, increases. It can also be seen that, under limited-capacity backhaul, the minimum total transmission power and the minimum number of repetitions of the QnF scheme converges to a constant for large K.

V. Conclusion

We studied the impact of multiple BSs and limited-capacity backhaul on NB-IoT preamble detection performance by using the stochastic geometry analysis. Numerical result shows the relative merits of these schemes. More specifically, our results show that DnF scheme outperforms QnF scheme when the backhaul capacity is limited or when the minimum distance between user and BSs is less than a threshold. Our result also shows that multiple BSs improve the preamble detection performance as well as reduce the number of repetition and the total power of the preamble transmission significantly.

Acknowledgment

This work has been partly performed in the framework of the Horizon 2020 project ONE5G (ICT-760809) receiving funds from the European Union. The views expressed in this work are those of the authors and do not necessarily represent the project view.

Appendix A

In this Appendix, we derive the mean and variance of $S(\gamma)$. It follows from (1) that we have

$$\mathrm{E}(d_k^{-\alpha}) = 2\frac{(r^{2-\alpha} - R^{2-\alpha})}{(\alpha-2)(R^2-r^2)}, \tag{36}$$

$$\mathrm{E}(d_k^{-2\alpha}) = \frac{(r^{2-\alpha} - R^{2-\alpha})}{(\alpha-1)(R^2-r^2)}, \tag{37}$$

respecitvely. Hence, since $J_k(\gamma)$ for $1 \leq k \leq K$ are independent, it follows from (4) and (5) that the mean and variance of $S(\gamma)$ can be obtained by

$$\mathrm{E}[S(\gamma)] = v\xi\sigma_n^2 KMp \times \mathrm{E}\left(1+\xi\gamma d_k^{-\alpha}\right) \tag{38}$$

$$= v\xi\sigma_n^2 KM_p\left(1+2\xi\gamma\frac{(r^{2-\alpha}-R^{2-\alpha})}{(\alpha-2)(R^2-r^2)}\right), \tag{39}$$

and

$$\begin{aligned}
&\mathrm{var}[S(\gamma)]\\
&= K \times \mathrm{var}[J_k(\gamma)] && (40)\\
&= K \times \{\mathrm{E}[\mathrm{var}(J_k(\gamma)|d_k)] + \mathrm{var}[\mathrm{E}(J_k(\gamma)|d_k)]\} && (41)\\
&= K(v\xi\sigma_n^2)^2\\
&\quad \times \left\{M_p\mathrm{E}[(1+\xi\gamma d_k^{-\alpha})^2] + M_p^2\mathrm{var}(1+\xi\gamma d_k^{-\alpha})\right\} && (42)\\
&= KM_p(v\xi\sigma_n^2)^2\left(1+4\xi\gamma\frac{(r^{2-\alpha}-R^{2-\alpha})}{(\alpha-2)(R^2-r^2)}\right)\\
&\quad + K(v\xi\sigma_n^2)^2(\xi\gamma)^2\Bigg(\frac{(M_p^2+M_p)(r^{2-2\alpha}-R^{2-2\alpha})}{(\alpha-1)(R^2-r^2)}\\
&\quad - \frac{4M_p^2(r^{2-\alpha}-R^{2-\alpha})^2}{(\alpha-2)^2(R^2-r^2)^2}\Bigg), && (43)
\end{aligned}$$

respectively, where the law of total variance is applied in (41).

APPENDIX B

In this Appendix, we prove that $\Pr(J_i(\gamma) > \lambda_{DnF}|\mathcal{D}_1^i)$ in (32) is a strictly decreasing function of r.

Taking the fist derivative of $\Pr(J_i(\gamma) > \lambda_{DnF}|\mathcal{D}_1^i)$ with respect to r yields

$$\begin{aligned}
&\frac{d\Pr(J_i(\gamma) > \lambda_{DnF}|\mathcal{D}_1^i)}{dr}\\
&= \Gamma\left(M_p, \frac{\lambda_{DnF}}{v\xi\sigma_n^2(1+\xi\gamma r^{-\alpha})}\right)\frac{2r}{R^2-r^2}\\
&\quad - \int_r^R \Gamma\left(M_p, \frac{\lambda_{DnF}}{v\xi\sigma_n^2(1+\xi\gamma x^{-\alpha})}\right)\frac{2r}{(R^2-r^2)^2}2xdx && (44)\\
&< \Gamma\left(M_p, \frac{\lambda_{DnF}}{v\xi\sigma_n^2(1+\xi\gamma r^{-\alpha})}\right)\frac{2r}{R^2-r^2}\\
&\quad - \Gamma\left(M_p, \frac{\lambda_{DnF}}{v\xi\sigma_n^2(1+\xi\gamma r^{-\alpha})}\right)\int_r^R\frac{2r}{(R^2-r^2)^2}2xdx && (45)\\
&= 0, && (46)
\end{aligned}$$

where the Leibniz integral derivative rule is applied to derive (44) and the inequality of

$$\Gamma\left(M_p, \frac{\lambda_{DnF}}{v\xi\sigma_n^2(1+\xi\gamma x^{-\alpha})}\right) > \Gamma\left(M_p, \frac{\lambda_{DnF}}{v\xi\sigma_n^2(1+\xi\gamma r^{-\alpha})}\right), \tag{47}$$

for all $x > r$ is applied to derive (45). Hence we have $d\Pr(J_i(\gamma) > \lambda_{DnF}|\mathcal{D}_1^i)/dr < 0$ i.e. $\Pr(J_i(\gamma) > \lambda_{DnF}|\mathcal{D}_1^i)$ in (32) is a strictly decreasing function of r.

REFERENCES

[1] M. R. Palattella, M. Dohler, A. Grieco, G. Rizzo, J. Torsner, T. Engel, and L. Ladid, "Internet of things in the 5G era: Enablers, architecture, and business models," *IEEE Journal on Selected Areas in Communications*, vol. 34, no. 3, pp. 510–527, 2016.

[2] O. Liberg, M. Sundberg, E. Wang, J. Bergman, and J. Sachs, *Cellular Internet of Things: Technologies, Standards, and Performance*. Academic Press, 2017.

[3] S. Sesia, M. Baker, and I. Toufik, *LTE-the UMTS long term evolution: from theory to practice*. John Wiley & Sons, 2011.

[4] X. Lin, A. Adhikary, and Y. P. E. Wang, "Random access preamble design and detection for 3GPP narrowband IoT systems," *IEEE Wireless Communications Letters*, vol. 5, pp. 640–643, Dec 2016.

[5] W. S. Jeon, S. B. Seo, and D. G. Jeong, "Effective frequency hopping pattern for ToA estimation in NB-IoT random access," *IEEE Transactions on Vehicular Technology*, pp. 1–1, 2018.

[6] T. Kim, D. M. Kim, N. Pratas, P. Popovski, and D. K. Sung, "An enhanced access reservation protocol with a partial preamble transmission mechanism in NB-IoT systems," *IEEE Communications Letters*, vol. 21, pp. 2270–2273, Oct 2017.

[7] L. Liu and W. Yu, "Massive connectivity with massive MIMO - Part I: Device activity detection and channel estimation," *IEEE Transactions on Signal Processing*, vol. 66, pp. 2933–2946, June 2018.

[8] Z. Utkovski, O. Simeone, T. Dimitrova, and P. Popovski, "Random access in C-RAN for user activity detection with limited-capacity fronthaul," *IEEE Signal Processing Letters*, vol. 24, no. 1, pp. 17–21, 2017.

[9] N. Jiang, Y. Deng, X. Kang, and A. Nallanathan, "Random access analysis for massive IoT networks under a new spatio-temporal model: A stochastic geometry approach," *IEEE Transactions on Communications*, 2018.

[10] M. Haenggi, R. K. Ganti, *et al.*, "Interference in large wireless networks," *Foundations and Trends® in Networking*, vol. 3, no. 2, pp. 127–248, 2009.

[11] M. Haenggi, *Stochastic geometry for wireless networks*. Cambridge University Press, 2012.

[12] S. Atapattu, C. Tellambura, and H. Jiang, *Energy detection for spectrum sensing in cognitive radio*. Springer, 2014.

[13] T. Stewart, L. Strijbosch, H. Moors, and P. v. Batenburg, "A simple approximation to the convolution of gamma distributions," 2007.

[14] P. K. Varshney, *Distributed detection and data fusion*. Springer Science & Business Media, 2012.